

## Improvement of eosin visible light degradation using PbS-sensitized TiO<sub>2</sub>

R. Brahimi<sup>a</sup>, Y. Bessekhouda<sup>a,b,\*</sup>, A. Bouguelia<sup>a</sup>, M. Trari<sup>a</sup>

<sup>a</sup> Faculty of Chemistry, U.S.T.H.B., BP 32, 16111 El-Alia, Algiers, Algeria

<sup>b</sup> National Veterinary School, BP 161, El-Harrach, Algiers, Algeria

Received 15 March 2007; received in revised form 5 August 2007; accepted 6 August 2007

Available online 11 August 2007

### Abstract

PbS was prepared by a simple chemical method for use as a photosensitizer with TiO<sub>2</sub>. Its physico-chemical characterisation reveals a semiconducting behaviour with a band gap energy of 0.41 eV showing efficient visible light absorption. The valence and conduction band energy levels are −0.78 and −1.19 V, respectively. Interparticle electron injection (IPEI) from photoactivated PbS to inactivated TiO<sub>2</sub> was demonstrated by the increase of eosin degradation under visible light. Different parameters affecting the photoactivity such as the PbS amount, eosin concentration and initial pH were investigated. Optimal degradation of eosin occurs at a PbS/TiO<sub>2</sub> ratio of 10:90, an eosin concentration of 30 mg l<sup>−1</sup>, a pH ~7, and when using a 2 × 200 W tungsten lamp. These conditions result in a constant decomposition rate of 0.116 min<sup>−1</sup> corresponding to an eosin half-life of 6.4 min. In this case, the rate of degradation of eosin is respectively 20 and 40 times greater than when in contact with pure TiO<sub>2</sub> or through direct photolysis.

The photoefficiency of PbS(10%)/TiO<sub>2</sub> was compared to that of CdS(10%)/TiO<sub>2</sub>, Bi<sub>2</sub>S<sub>3</sub>(10%)/TiO<sub>2</sub>, Cu<sub>2</sub>O(10%)/TiO<sub>2</sub> and Bi<sub>2</sub>O<sub>3</sub>(10%)/TiO<sub>2</sub> using visible and UV–vis light. PbS(10%)/TiO<sub>2</sub> has the best efficiency regardless of the wavelength of light used. The contribution of the electromotive force and the band gap of the narrow band gap semiconductor to the photoactivity improvement were discussed.

© 2007 Elsevier B.V. All rights reserved.

**Keywords:** PbS; TiO<sub>2</sub>; Narrow band gap semiconductors; Heterojunctions; IPEI; Eosin; Photocatalytic degradation

### 1. Introduction

Photocatalytic degradation of organic pollutants and organic dyes using semiconductors (SC) such as TiO<sub>2</sub> continues to attract interest as a method to mitigate their impact on the environment [1–3]. Dyes in particular contribute to eutrophication of water supplies and their incomplete photodegradation can also lead to production of carcinogenic intermediate molecules depending on the wavelength of the incident light [4–6].

TiO<sub>2</sub> is a well-known wide band gap semiconductor ( $E_g \sim 3.2$  eV) and as a consequence can aid in dye degradation using UV light with the dye acting as both a sensitising agent and pollutant. However, the rate of degradation remains very low and the process is restricted to organic dyes whose lowest unoccupied molecular orbital (LUMO) is lower in energy than the conduc-

tion band (CB) energy of TiO<sub>2</sub>. The low degradation efficiency of TiO<sub>2</sub> can be ascribed to charge recombination between the electrons injected into CB-TiO<sub>2</sub> and the oxidized sensitizer, a situation also often observed in solar cells (n-DSC) [7,8]. Another problem with such degradation processes is buildup of colourless by-products whose degradation competes with the dye itself by adsorbing preferentially to TiO<sub>2</sub> surface and preventing electron injection phenomena [1].

All of these drawbacks to TiO<sub>2</sub> degradation of organic dyes can be resolved by mixing a narrow band gap SC into TiO<sub>2</sub> as a sensitizer. The narrow band gap SC is able to generate and inject electrons through the CB of wide band gap SC (TiO<sub>2</sub>) without actually binding to the surface of the TiO<sub>2</sub>. This remote charge injection is possible by virtue of an electromotive force generated by the difference between the CBs of both the wide and narrow band gap semiconductors.

Recently, different heterosystems such as CdS/TiO<sub>2</sub>, Bi<sub>2</sub>S<sub>3</sub>/TiO<sub>2</sub>, Bi<sub>2</sub>O<sub>3</sub>/TiO<sub>2</sub>, Cu<sub>2</sub>O/TiO<sub>2</sub> [9–11] have been studied for their potential application to photocatalytic degradation of organic pollutants. The heterojunctions were investigated under

\* Corresponding author at: Faculty of Chemistry, U.S.T.H.B., BP 32, 16111 El-Alia, Algiers, Algeria. Tel.: +213 70327993; fax: +213 21247311.

E-mail address: [ybessekhouda@yahoo.fr](mailto:ybessekhouda@yahoo.fr) (Y. Bessekhouda).

different conditions of irradiation, using visible and UV–vis light as well as several different pollutants (dye, aromatic ring containing acidic or basic functional groups). The results suggest that the efficiency of the heterojunction can be maximized by a judicious choice of the narrow band gap SC with high visible light absorption and adequate CB position being the most important properties for consideration.

Recently, the photoelectrochemical properties of the PbS/TiO<sub>2</sub> heterojunction were reported to exhibit relatively high photoconversion efficiency [12,13]. High efficiencies suggest that this heterojunction may also exhibit high efficiency in degradation of organic dye and pollutants using visible light. Here we evaluate the suitability and efficiency of the PbS/TiO<sub>2</sub> heterojunction for its use in decomposing organic pollutants by examining the physico-chemical properties of PbS and correlating these properties with the photoefficiency of the heterojunction with TiO<sub>2</sub>.

Eosin (EOS) was used as a model molecule for investigating mechanisms of degradation under a variety of conditions. The PbS/TiO<sub>2</sub> system was compared to other heterojunctions previously studied [9,10] using both visible and UV–vis irradiation providing an overview of the contribution of the electromotive force and the band gap energy to the performance enhancement of the heterojunctions.

## 2. Experimental

PbS was prepared by a direct precipitation process in which Pb(NO<sub>3</sub>)<sub>2</sub> was added drop wise to an alkaline solution containing Na<sub>2</sub>S until a 1:1 molar ratio of Pb<sup>2+</sup> and S<sup>2-</sup> was reached. The resulting precipitate and solution was heated at 80 °C for 1 h, filtered, washed several times with distilled water and then acetone and was then dried at 110 °C overnight. The resulting black powder was heated at 250 °C for 1 h. TiO<sub>2</sub> was purchased from Degussa (TiO<sub>2</sub>-P25) and used as received. CdS, Bi<sub>2</sub>S<sub>3</sub>, Bi<sub>2</sub>O<sub>3</sub> were prepared according to procedures detailed earlier [9,10], whereas Cu<sub>2</sub>O was supplied from Aldrich and used as received. The heterojunctions were obtained by direct mixing of the constituents.

The band gap of PbS was obtained by FTIR analysis using 1 mg of PbS dispersed in 150 mg of spectroscopic grade KBr which was then mixed in a mortar and sintered to obtain a pellet of 0.5 mm of thickness. The spectra were obtained in both absorbance and reflectance modes.

The powder X-ray diffraction (XRD) pattern of PbS was obtained with a Philips diffractometer equipped with a monochromated high intensity Cu K $\alpha$  ( $\lambda = 1.5405 \text{ \AA}$ ) in the scan range  $2\theta$  (20–80°).

Absorption and reflectance spectra of PbS were recorded with Fourier transform infrared spectrophotometer (Bio-Rad-FTS 3000MX) in the spectral range 2500–5000 nm.

The thermal variation conductivity  $\sigma$  of PbS was measured through the dc electrical conductivity by the two-terminal method using equipment described elsewhere [14]. PbS was prepared as sintered pellets which were heated at 400 °C in evacuated Pyrex tube during 1 h to obtain a compactness of 85%.

Electrochemical measurements were performed in 1 M KOH (pH  $\sim$ 13.6) and in 1 M KCl (pH  $\sim$ 7.1) using a “three electrode device” with a PbS working electrode, a large platinum counter electrode and a saturated calomel reference electrode (SCE). The electrolyte was continuously flushed with pure nitrogen gas. The intensity–potential  $J(V)$  characteristics were recorded with a PGP201 Voltalab potentiostat. A 200 W Oriel (model 66183) tungsten lamp was used as light source. The flux intensity ( $28.632 \text{ mW cm}^{-2}$ ) was determined by a light-meter (Testo 545). Photocurrent–photovoltage ( $J_{ph}$ – $U_{ph}$ ) plots were obtained using a two electrode cell equipped with external adjustable resistance permitting tuning of the resistivity.

Photocatalytic experiments were performed using two 200 W tungsten lamps as visible light sources (UV-free radiation) placed horizontally to the reactor. The reactor was surrounded by a double walled Borosilicate water cooling jacket for temperature control. For each experiment, 250 ml of solution was used with a 5 ml aliquot which was taken out at regular intervals for analysis. Eosin (EOS) was used as representative organic dye molecule. Samples containing the catalyst were centrifuged prior to analysis with a UV–vis spectrophotometer Cary 50 Con. ( $\lambda_{max} = 516 \text{ nm}$ ). Identical experiments were also carried out with a 300 W halogen-tungsten lamp to explore the effects of the addition of UV radiation to the heterojunction behavior. UV radiation was occasionally removed using an optical filter of poly(methyl methacrylate) (PMMA) with a thickness of 10 mm for selected investigations.

## 3. Results and discussion

### 3.1. PbS characterization

Fig. 1 shows the powder XRD pattern of PbS after heat-treatment at 250 °C. All the peaks were indexed according to JCPDS card (5-0592) indicating single phase formation. PbS crystallized in a face centered cubic system (rock salt NaCl structure). The cell parameter ( $a = 0.5945 \text{ nm}$ ) was determined from the most intense peak (2 2 0), which is in good agreement with that reported in the literature [15]. The crystallite size was determined from the Scherrer formula using the full-width at half-maximum (FWHM) of the peak (2 2 0) taking into account

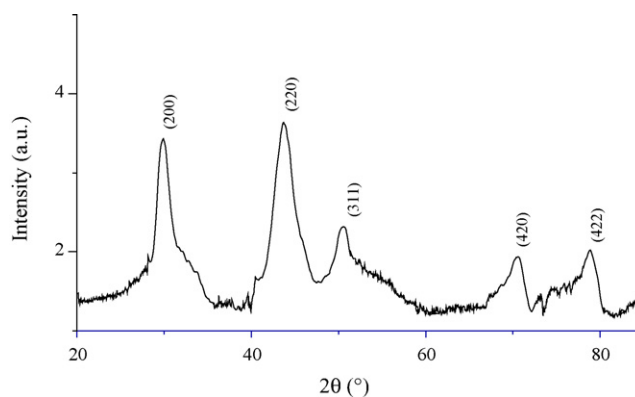


Fig. 1. X-ray diffraction pattern of PbS synthesized via co precipitation.

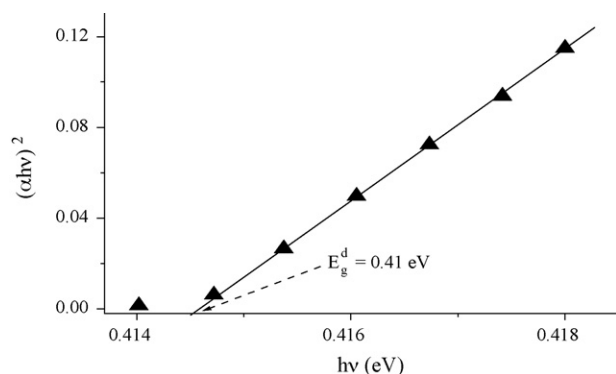


Fig. 2. Direct band gap transition of PbS.

the instrument broadening. A crystallite size average of 4 nm was obtained.

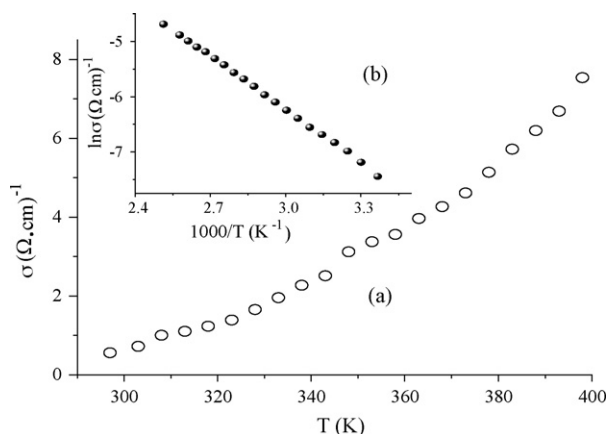
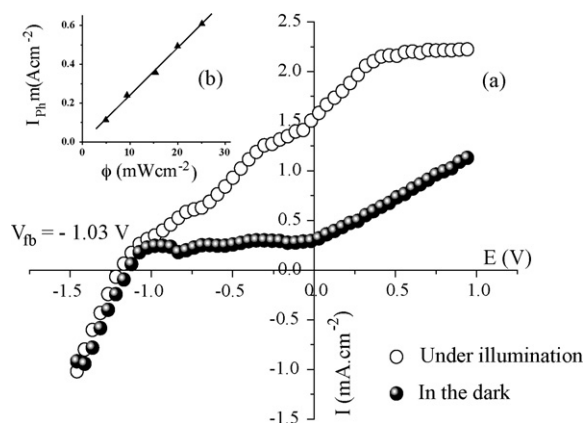
Because of its black color, the band gap energy ( $E_g$ ) of PbS was determined using FTIR analysis. The absorption coefficient ( $\alpha$ ) was calculated using the following equation [16]:

$$\alpha \propto \left(\frac{1}{t}\right) \log \left(\frac{I_0}{I_t}\right)$$

where  $I_0$  is the incident intensity and  $I_t$  is the intensity after traveling the thickness  $t$  of the pellet and  $I_0/I_t$  can be considered as the absorbance.

$E_g$  was determined by plotting  $(\alpha h\nu)^n$  versus  $h\nu$  and extrapolating the linear portion which intercepts the energy axis  $h\nu$ . The exponent  $n$  can take the value 1/2 or 2, respectively for indirect and direct optical transition. An  $E_g$  value of 0.41 eV was obtained which corresponds to a direct optical transition, i.e.,  $n=2$  (Fig. 2). This result suggests that PbS can be easily activated by visible light.

Fig. 3a shows the temperature dependence of the electrical conductivity of PbS in the temperature range of 298–400 K; covering the thermal stability of PbS. As observed, PbS exhibits a semiconducting behavior. The temperature dependence of  $\sigma$  can be fitted to the usual Arrhenius equation:  $\sigma = \sigma_0 \exp(-\Delta E_\sigma/RT)$  where  $\sigma_0$  is the pre-exponential factor and  $\Delta E_\sigma$  the activation energy. The linearization of this equation in the form of  $\ln \sigma$

Fig. 3. Temperature dependence of the electrical conductivity ( $\sigma$ ) for PbS (a).  $\ln(\sigma)$  vs.  $1000/T$  (b).Fig. 4. The  $J(V)$  characteristics of PbS in 1 M KOH both in the dark and under visible illumination (a). The linear variation of the photocurrent vs. the light intensity curve in 1 M KOH solution (b).

versus  $1000/T$  yields  $\Delta E_\sigma$  of 0.25 eV (Fig. 3b). This suggests that conduction occurs through a thermal activation mechanism where the conductivity increases with temperature.

The flat band potential ( $V_{fb}$ ) was determined by plotting  $J$ – $V$  curves both in the dark and under illumination (Fig. 4a). The increase of the photocurrent ( $J_{ph}$ ) towards the anodic direction confirms the n-type conductivity of PbS. In KOH media  $J_{ph}$  starts to flow at a potential  $V_{ON}$  of  $-1.03$  V and increases until saturation. The potential  $V_{ON}$  can be reasonably considered as  $V_{fb}$  which corresponds to the position of the Fermi level.  $J_{ph}$  depends linearly on the light intensity ( $\phi$ ) as expected ( $J_{ph} = a\phi$ ,  $a = 23.6$  mA/W) (Fig. 4b). This fact leads us to think that the rate of the recombination process is low and all the generated charge carriers contribute to the photocurrent. The pH effect on the potential  $V_{fb}$  was also investigated by performing the experiment using KCl (1 M) instead of KOH (1 M) and the results show that  $V_{fb}$  is pH-insensitive. The fill factor (FF) that represents the ideality of the PEC system was investigated in KCl media. FF is given by the following equation:

$$FF = \frac{J_m U_m}{J_{sc} V_{oc}}$$

where  $J_m$  and  $U_m$  can be obtained by computing the product at various points along the plot and selecting the point that gives the higher product corresponding to the useful maximal power.  $J_{sc}$  and  $V_{oc}$  are, respectively the short circuit current and the open circuit voltage. FF must be close to unity for an efficient PEC cell in the ideal case. In our case FF value of 0.34 was obtained with a light intensity of  $28 \text{ mW cm}^{-2}$  (Fig. 5).

The low FF can be attributed to the fact that the solution does not contain any hole scavenger and/or to the low conductivity as well as grains boundaries. Indeed, the absence of hole scavenger decreases the efficiency of the charge separation and the life time of charge carriers. The low FF value is a good indicator of the capability of PbS to operate as a photocatalyst without itself being sacrifice.

Combining the above physical characteristics ( $E_g$ ,  $\Delta E_\sigma$ ,  $V_{fb}$ ) (Table 1) allows us to build the energetic band diagram for PbS and to compare it to that of  $\text{TiO}_2$  and EOS (Fig. 6). According to the respective conductive band positions of both semicon-

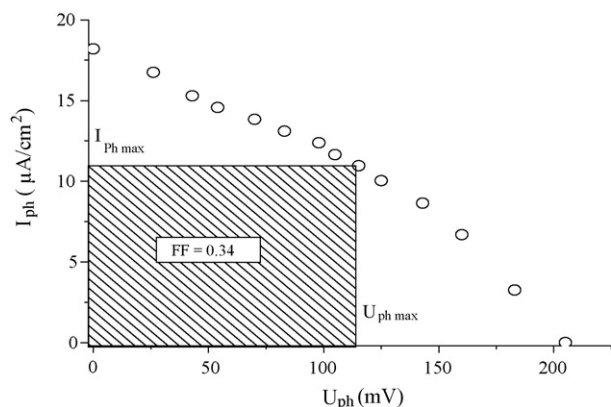


Fig. 5. Photocurrent–photovoltage characteristic for PbS in 0.1 M KCl solution at pH ~7 under visible light.

Table 1  
Some physico-chemical properties of PbS

$a$ (nm)	0.5945
$d$ (nm)	~4
$E_g$ (eV)	0.41
$\sigma$ ( $\Omega \text{ cm}$ ) <sup>-1</sup>	$5.6 \times 10^{-4}$
$\Delta E_\sigma$ (eV)	0.25
$V_{fb}$ (V)	-1.03
FF	0.34
BV (V)	-0.78
BC (V)	-1.19

ductors, an effective photosensitization of TiO<sub>2</sub> by PbS can be envisaged. It is important to note that the PbS/TiO<sub>2</sub> heterojunction (photoelectrode) was studied using visible light and showed an interesting photocurrent production demonstrating interparticle electron transfer [12,13]. However, there is no explanation, to our knowledge, of the phenomena that take into account the energetic band position of PbS.

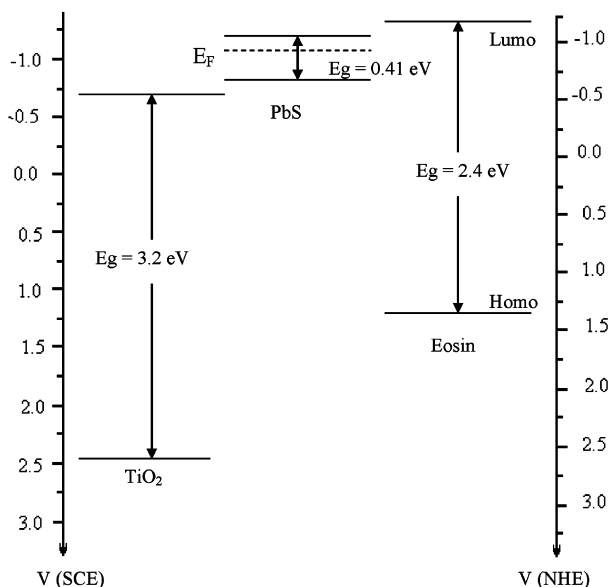


Fig. 6. The energy band diagram of PbS/TiO<sub>2</sub> heterojunction in eosin solution at pH ~7.

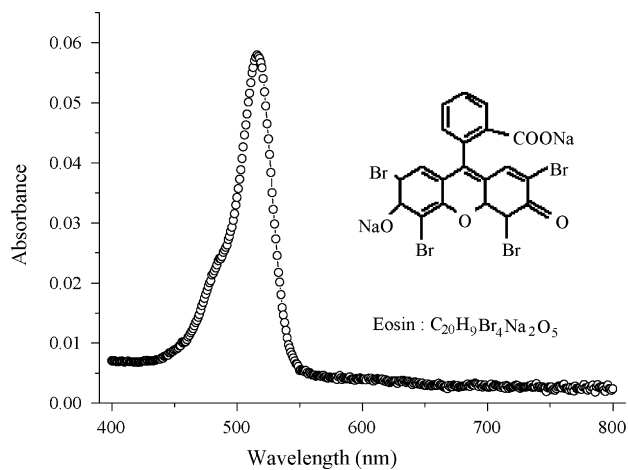


Fig. 7. Visible absorption spectrum and molecular structure of eosin.

### 3.2. Photocatalytic efficiency of PbS/TiO<sub>2</sub> heterojunction

The photocatalytic performance of PbS/TiO<sub>2</sub> was investigated using eosin (EOS) as representative molecule. The absorption spectra and chemical structure of EOS are depicted in Fig. 7. It should be noted that EOS degradation by direct photolysis (in a catalyst-free media) follows pseudo zero-order kinetics. When TiO<sub>2</sub> or PbS/TiO<sub>2</sub> were used, the disappearance of EOS follows first-order kinetics at natural pH ~7. The photocatalytic efficiency over the heterojunction was compared, in each case, to that of TiO<sub>2</sub> alone and to direct photolysis under visible irradiation.

#### 3.2.1. Effect of PbS concentration

The study of the effect of PbS on the activation of TiO<sub>2</sub> under visible light was performed by varying the mass of PbS while keeping the mass of TiO<sub>2</sub> (125 mg) constant. Here we report this variation as a percentage of PbS with respect to the total mass of catalyst. Fig. 8 shows how the amount of PbS affects photocatalytic EOS degradation. The efficiency of the heterojunction produced by mixing PbS with TiO<sub>2</sub> strongly depends

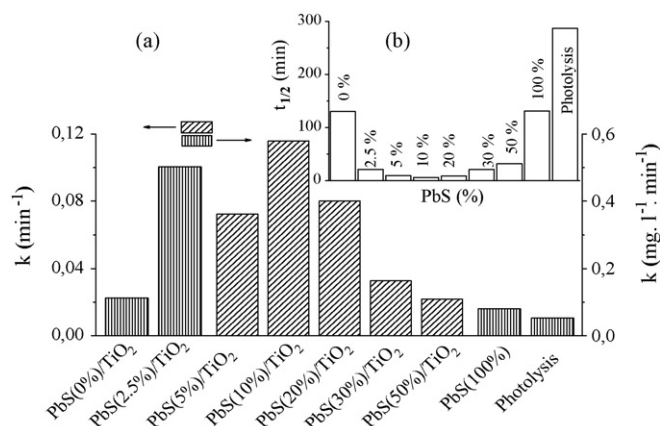


Fig. 8. (a) Effect of PbS concentration toward the photocatalytic activity of PbS(%) / TiO<sub>2</sub> heterojunction, (b) half-life of eosin over PbS concentration; experimental conditions: eosin initial concentration: 30 mg l<sup>-1</sup>, volume of the solution: 250 ml, light source: tungsten lamp 2 × 200 W, initial pH ~7.



on the PbS amount. The best configuration, obtained using 10% of PbS, results in an EOS half-life of 6.4 min. The degradation rate in this case is respectively, 20 and 40 times greater than that of pure  $\text{TiO}_2$  and direct photolysis of EOS.

From a mechanistic point of view, it should be noted that when EOS is irradiated by visible light, excitation of the dye occurs by promotion of an electron from the HOMO band (0.96/SCE) to the LUMO band ( $-1.34/\text{SCE}$ ) [17] which goes on to react with dissolved oxygen to generate  $\text{O}_2^{\bullet-}$ . This oxygen radical reacts with EOS itself via a complex mechanism that results in the destruction of EOS molecules. This mechanism is inefficient as the charges are lost by internal filtration and are not sufficiently separated physically due to the absence of sufficiently high electric junction field. This problem can be partially resolved by dispersing  $\text{TiO}_2$  in the solution. When the adsorbed dye is excited, electrons are generated and subsequently injected into the CB- $\text{TiO}_2$  which goes on to produce oxygen radicals. The potential difference between LUMO of EOS and CB- $\text{TiO}_2$  leads to a better charge separation than in the case of photolysis of EOS alone. The phenomenon as described is believed to occur only when adsorption of EOS onto  $\text{TiO}_2$  surface remains low (<3%).

The specific role of pure PbS in increasing of EOS degradation efficiency is still unclear. It should be noted that under our experimental conditions, about 25% of EOS is adsorbed. Nevertheless, the half-life of EOS using PbS is roughly the same as in the case of  $\text{TiO}_2$  (~130 min). The idea that PbS plays an important role in promoting charge separation, but not on direct radical generation on their surface was suggested on the basis of two experiments. In the first experiment, attempted photodegradation of the colorless chemicals benzamide or 4-hydroxybenzoic [1] using a pure PbS fails. This indicates that PbS alone is not able to generate radicals. In the second experiment, photocurrent measurements using PbS electrode at 0.5 V/ECS and under varying concentrations of EOS showed not only that the photocurrent is insensitive to the EOS concentration but also to the absence and presence of EOS. This result indicates that EOS does not participate in the photocurrent generation and as a consequence the electron injection phenomena previously described cannot occur. Taking into account the results of the photoactivity and the investigation of the role of PbS, we can assume that PbS plays an effective role in improving charge separation but that the generation of radicals is not through its conduction band. At this stage, it is clear that the mechanism of the photoefficiency improvement in the case of PbS is different than that of  $\text{TiO}_2$  although its exact role is ambiguous.

Ideal photodegradation was obtained by mixing PbS and  $\text{TiO}_2$  together to produce a heterojunction. Using visible light, PbS acts as an optical harvesting particle and the electrons present in its CB are physically transferred through the CB- $\text{TiO}_2$  to generate radicals. The interparticle electron transfer behavior combined with the electron injection of the dye lead to the efficient production of radicals that results in high photocatalytic activity. Due to the fact that interparticle electron transfer occurs only when both SCs are in intimate contact, the probability of particle collision then governs the photocatalytic efficiency of the heterojunction. The ratio of PbS must be sufficiently high for improving particle collision and thus generation and inter-

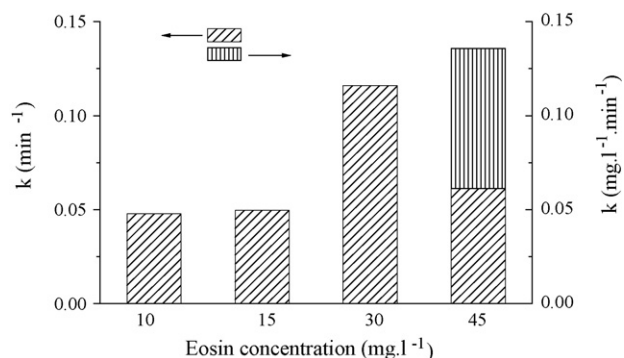


Fig. 9. Effect of eosin initial concentration toward PbS(10%)/ $\text{TiO}_2$  photoactivity, experimental conditions—mass of the heterojunction: 138.88 mg, volume of the solution: 250 ml, light source: tungsten lamp  $2 \times 200$  W, initial pH ~7.

particle electron transfer. This works up to a critical point (in our case 10%) after which, increasing the PbS ratio leads to charge loss by itself acting as recombination center.

### 3.2.2. Effect of eosin concentration

The study of the effect of EOS concentration on the photocatalytic performance of the PbS(10%)/ $\text{TiO}_2$  heterojunction shows a maximum efficiency at EOS concentration close to  $30 \text{ mg l}^{-1}$ . The rate of EOS decolorization increases with EOS concentration until  $30 \text{ mg l}^{-1}$  (Fig. 9) and is intimately connected to radical generation on the catalyst surface and to the probability of subsequent radical reaction with dye molecules. When EOS concentration increases, the probability of reaction between EOS and oxidizing species increases and leads to an improvement of the degradation rate. However, EOS excess induces a decrease of the degradation rate, possibly for one of the following reasons: (i) excess EOS may act as an optical filter by itself absorbing photons otherwise destined to be absorbed by the heterojunction; (ii) abundant EOS molecules might occupy active sites for radical production on the catalyst surface, thereby blocking radical generation; (iii) high dye concentration may lead to accumulation of intermediate molecules which, at a critical concentration, compete effectively with the decolorization process. In our case, all the mentioned effects are suspected to occur. For EOS concentration of  $45 \text{ mg l}^{-1}$ , the kinetic of decolorization showed three distinguishable phases. In the first phase, a kinetic of pseudo zero-order ( $k = 0.1358 \text{ mg l}^{-1} \text{ min}^{-1}$ ) is observed indicating that the photolysis mechanism (*i.e.*, the reaction between radicals and dye occurs within the solution) governs the degradation process. After 100 min the decolorization stopped as intermediate products of degradation began to compete effectively for radicals. This phase lasts for approximately 60 min before degradation begins again, but in this case with apparent first-order kinetics ( $k = 0.0612 \text{ min}^{-1}$ ). The degradation process is assumed mainly to occur at the semiconductor–electrolyte interface.

### 3.2.3. Effect of pH

To study the effect of pH on the photocatalytic efficiency of PbS(10%)/ $\text{TiO}_2$ , the pH was adjusted between 4 and 10. As EOS carboxylate functional groups are not protonated [18], the absorption properties of EOS remain practically invariant in this

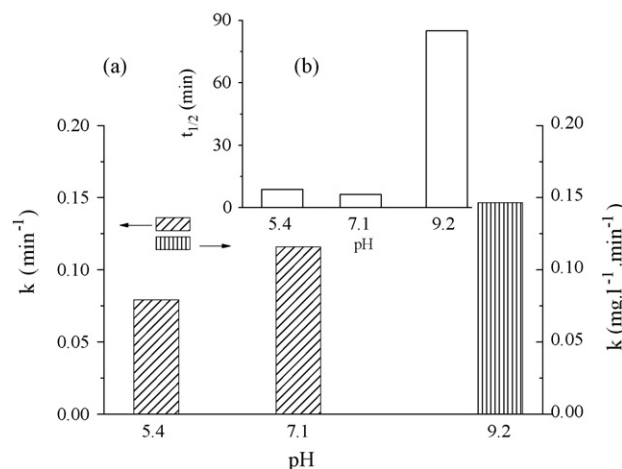


Fig. 10. (a) Effect of the initial pH toward the photocatalytic efficiency of PbS(10%)/TiO<sub>2</sub> heterojunction, (b) half-life of eosin versus the initial pH; experimental conditions—mass of the heterojunction: 138.88 mg, eosin initial concentration: 30 mg l<sup>-1</sup>, volume of the solution 250 ml, light source: tungsten lamp 2 × 200 W.

range and any change in the photocatalytic efficiency cannot be ascribed to the structure variation of EOS. Fig. 10 shows that the pH of the solution plays a crucial role on the photocatalytic efficiency of the heterojunction. In alkaline media (pH ~9.2), a strong deactivation was observed accompanied by a change to zero-order kinetics ( $k = 0.1464 \text{ mg l}^{-1} \text{ min}^{-1}$ ). By contrast, for acidic media (pH ~5.4), the rate of degradation was greater than in the case of basic media but remained unfortunately lower than that observed at neutral pH (~7) even though the half-life of the dye in both cases (*i.e.* acidic and neutral pHs) are very close. It should be noted that in acidic solution, adsorption of EOS was very high (47% of initial EOS concentration) in contrast with basic media in which no adsorption was observed. Taking into account the  $\text{pH}_{\text{pzc}}$  (~6.8) of commercial TiO<sub>2</sub>-P25 [19], the active surface is negatively charged in basic pH leading to a strong electrostatic repulsion with the dye molecule in dianionic form. In this respect, the degradation process does not take place over the TiO<sub>2</sub> surface but certainly in the bulk solution or close to the surface. Due to the very short lifetime of radicals, a signif-

icant number are lost during their migration inducing a drastic decrease of the efficiency. Direct EOS photolysis efficiency was almost pH-insensitive in the studied range. If we compare the half-life of the dye using the heterojunction (85 min) with that of direct photolysis (239 min) at the same pH (~9.2), the difference in the half-lives suggests that the heterojunction plays the main role in radical generation, regardless of the adsorption of EOS on TiO<sub>2</sub> surface.

Unlike in alkaline solution, TiO<sub>2</sub> surface in acidic media is positively charged leading to a strong EOS adsorption which favors the electron injection phenomena. One would expect that in these conditions the degradation efficiency of the heterojunction should increase drastically due the accumulation of electrons in CB-TiO<sub>2</sub> as a result of the sensitization of TiO<sub>2</sub> by PbS and EOS. This was not observed suggesting that the resulting mechanism is not synergic but favors instead the loss of charges by recombination. Using PbS, a  $\text{pH}_{\text{pzc}}$  of 6.74 leads to the same adsorption behavior as TiO<sub>2</sub>. However, due to the fact that the degradation process and dye sensitization take place only on TiO<sub>2</sub>, the effect of pH on the PbS when it forms a heterojunction cannot be considered as a determinant agent.

### 3.2.4. PbS/TiO<sub>2</sub> efficiency over other heterojunctions

The photocatalytic activity of the following heterojunctions were studied: PbS(10%)/TiO<sub>2</sub>, Bi<sub>2</sub>S<sub>3</sub>(10%)/TiO<sub>2</sub>, CdS(10%)/TiO<sub>2</sub>, Cu<sub>2</sub>O(10%)/TiO<sub>2</sub>, Bi<sub>2</sub>O<sub>3</sub>(10%)/TiO<sub>2</sub>. The experiment was performed under the same conditions used for the optimization of PbS/TiO<sub>2</sub>, except that a halogen-tungsten lamp (300 W) was used as a light source. UV irradiation was removed using an optical filter for performing the experiment under visible light. In each case, the amount of narrow band gap semiconductors was kept at the optimum concentration observed for PbS which was 10% of the total heterojunction mass. The photoactivity results are reported in Table 2 together with the electromotive forces (emfs) and the energy absorbance characteristic of each system.

Using visible light, photoactivity increased as the emf decreased, except for PbS(10%)/TiO<sub>2</sub> in which the best photoactivity was observed. It should be kept in mind that each

Table 2  
Heterojunctions photoactivity under visible and UV-vis light, and related properties

	TiO <sub>2</sub>	PbS(10%)/TiO <sub>2</sub>	Bi <sub>2</sub> S <sub>3</sub> (10%)/TiO <sub>2</sub>	CdS(10%)/TiO <sub>2</sub>	Cu <sub>2</sub> O(10%)/TiO <sub>2</sub>	Bi <sub>2</sub> O <sub>3</sub> (10%)/TiO <sub>2</sub>	EOS
<b>Visible light<sup>a</sup></b>							
$t_{1/2}$ (min)	218	16	83	206	269	78	332
Kinetic order	0	1	0	0	0	0	0
$K$ (mg l <sup>-1</sup> min <sup>-1</sup> )	0.0619	0.0419 <sup>b</sup>	0.161	0.0684	0.0514	0.103	0.047
Absorbed energy (eV)	2.4 <sup>c</sup>	0.4	1.3	2.4	2.2	2.7	2.4
emf (eV)	0.26	0.54	0.26	0.45	1.04	–	–
<b>UV-vis light<sup>d</sup></b>							
$t_{1/2}$ (min)	162	28	29	148	308	142	303
Kinetic order	0	0	0	0	0	0	0
$K$ (mg l <sup>-1</sup> min <sup>-1</sup> )	0.089	0.364	0.490	0.104	0.048	0.094	0.049

<sup>a</sup> Halogen-tungsten lamp of 300 W equipped with PMMA filter as a light source.

<sup>b</sup> Min<sup>-1</sup> unit due to kinetic order.

<sup>c</sup> Correspond to the absorbance energy of EOS.

<sup>d</sup> Halogen-tungsten lamp of 300 W as a light source.

heterojunction has its own specific absorbance properties. Visible light absorbance is dominated by EOS in the case of pure  $\text{TiO}_2$  and by the narrow semiconductor band gap in the case of the heterojunctions. If we compare the CdS- and  $\text{Cu}_2\text{O}$ -based junctions, the band gaps are close to one another while the emfs are very different. According to the observed photoefficiency, the junction that possesses the lowest emf has the highest efficiency indicating a connection between emf and electron transfer kinetics. Comparing PbS and CdS junctions in which the emf values are very close shows that the heterojunction which possesses the highest absorbance capacity has the best photoactivity, *i.e.*,  $\text{PbS}(10\%)/\text{TiO}_2$ . This fact demonstrates that although the emf is perhaps more important, the absorbance capacity cannot be neglected. Comparing the most efficient heterojunction ( $\text{PbS}/\text{TiO}_2$ ) and that is based on  $\text{Bi}_2\text{S}_3$  reveals that a higher emf can be compensated easily by a high absorbance capacity. With visible light in which only the narrow semiconductor is active in the heterojunction, the combination of a sufficiently low emf to improve the kinetic of electron transfer and a sufficiently high absorbance capacity to harvest sufficiently visible light is required in order to obtain the highest photocatalytic efficiency.

Using UV–vis lamp without an optical filter, both narrow band gap semiconductors and  $\text{TiO}_2$  are photoactive by themselves. One would therefore expect an increase in photoactivity with inclusion of UV radiation in the heterojunction system. However, the heterojunctions possessing an emf greater than 0.5 eV showed a decrease in photoactivity while those with an emf lower than 0.5 eV showed an increase upon inclusion of UV radiation. In the first case, the activation of  $\text{TiO}_2$ , and as a consequence the accumulation of electrons in its conduction band, seems to inhibit the electron injection phenomena occurring between narrow band gap semiconductor and  $\text{TiO}_2$ . This leads to a decrease in the heterojunctions photoactivities. On the other hand, the heterojunctions that have emf lower than 0.5 eV and a higher rate of electron transfer are not perturbed by the activation of  $\text{TiO}_2$ . Therefore, a better photoactivity using UV–vis light is obtained.

The best photoactivity of all junctions is invariably achieved by  $\text{PbS}(10\%)/\text{TiO}_2$  regardless of conditions, confirming the superior opto-electronic properties of this particular heterojunction.  $\text{PbS}(10\%)/\text{TiO}_2$  heterojunction showed a better efficiency under visible light than under UV–vis light. In contrast,  $\text{Cu}_2\text{O}(10\%)/\text{TiO}_2$  showed a poor photoactivity. This might be because its concentration was not optimized and was too low for efficient electron injection or because EOS interacts with the heterojunction resulting in charge loss.

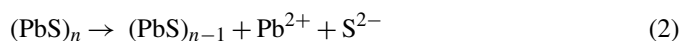
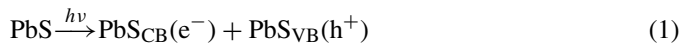
The general conclusion of this comparison both under visible and UV–vis light is that the selection of a narrow band gap semiconductor for building an efficient heterojunctions should take into account the following conditions:

- 1 The narrow band gap semiconductor must be the strongest absorber of visible light.
- 2 The emf of the heterojunction must be sufficiently low to permit swift electron transfer kinetics, with a critical value of approximately 0.5 eV.

- 3 The heterojunction selection should take into account both physical properties of the junction and those of the target molecule for degradation.

### 3.2.5. PbS stability

The chemical stability of PbS was investigated by dispersing the powder ( $0.696 \text{ g l}^{-1}$ ) in aqueous solution at pH  $\sim 7$  for 35 days once in the dark and once exposing the PbS to 6 h of irradiation (200 W) per day. When the vessel was maintained in the dark, a total drop of  $\text{Pb}^{2+}$  of  $0.097 \text{ g l}^{-1}$  was determined using inductively coupled plasma. At the end of this experiment, white particles were observed probably due to the formation of  $\text{Pb}(\text{OH})_2$  according to the solution pH. In the case of radiation exposure  $\text{Pb}^{2+}$  amounted to  $0.074 \text{ g l}^{-1}$ . This value is very low in comparison to the experiment in the dark and would seem to indicate that PbS is more stable under irradiation. However, the low  $\text{Pb}^{2+}$  concentration might also be attributed to  $\text{Pb}^{2+}$  reduction by electrons generated under light activation according to the following equations:



Although  $\text{PbS}(10\%)/\text{TiO}_2$  heterojunction exhibits a desirable photocatalytic activity its stability whether irradiated or not is a serious problem. Because of this,  $\text{PbS}(10\%)/\text{TiO}_2$  is a good model for advancing understanding of the mechanism and the properties required for an efficient visible and/or UV–vis light heterojunction configuration rather than as a practical junction ready for large scale use.

## 4. Conclusion

PbS was prepared by a direct precipitation process. XRD analysis showed a single phase formation and a crystallization in a face centered cubic system. A crystallite size averaging 4 nm was obtained. An  $E_g$  value of 0.41 eV was obtained which results from a direct optical transition. PbS exhibits a semiconducting behavior with an activation energy  $\Delta E_\sigma$  equal to 0.25 eV. The photoelectrochemical study allowed us to determine a flat band  $V_{\text{fb}}$  of  $-1.03 \text{ V}$  and a fill factor FF of 0.34. This study proved the absence of a hole scavenger which induces the decrease of charge separation efficiency and the life time of charge carriers.

Combining the physical characteristics ( $E_g$ ,  $\Delta E_\sigma$ ,  $V_{\text{fb}}$ ) allowed us to build the energetic diagram of PbS and to compare it to that of  $\text{TiO}_2$  and eosin predicting the electron injection phenomena. This behavior was confirmed by the photocatalytic activity observed under visible light. The very best heterojunction configuration was obtained with 10% of PbS. It was observed that the probability of particle-collision governs the photocatalytic efficiency and the excess of PbS induces charges lost by acting as recombination centers. An optimal value of  $30 \text{ mg l}^{-1}$  was found to be the ideal EOS concentration for photodegradation. At lower concentrations, accumulation of intermediates induces a competition with the decolorization pro-

cess. The effect of pH on the photoactivity showed a strong dependence on the eosin adsorption. Eosin adsorption depends on the charge type in the catalyst surface. Synergism between the photosensitization of eosin and the interparticle electron transfer was unfortunately not observed.

The comparison between PbS(10%)/TiO<sub>2</sub> and other heterojunctions having a range of band gaps and emf values helped to identify criteria for choosing suitable heterojunctions for photodegradation applications. Heterojunctions should include narrow band gap semiconductor that is the major absorber of visible light and the emf of the heterojunction must be sufficiently low to allow for fast electron transfer kinetics to obtain a high photoactivity in both visible light and UV–vis wavelength regimes. In addition, selection of heterojunction should take into account both absorption properties and type of the molecule to be degraded. After comparison, PbS(10%)/TiO<sub>2</sub> remains the best configuration for EOS degradation under visible light.

The stability of PbS is highly improved under irradiation due to the reduction of Pb<sup>2+</sup> generated by corrosion. However, even with such interesting results, to the use of such heterojunction for water treatment remains very improbable due to contamination risk with Pb<sup>2+</sup> even at low concentration. In spite of this, PbS remains a robust model of optoelectronic properties of an efficient heterojunction with TiO<sub>2</sub>. Efforts must be taken to improve our understanding of the heterojunction applications and to find semiconductors that have properties close to that of PbS but that are harmless to the environment.

### Acknowledgement

The authors would like to thank Dr. Tom Custer from Max-Planck Institute for Chemistry in Mainz, Germany for the English improvement of the manuscript.

### References

- [1] Y. Bessekhoud, D. Robert, J.-V. Weber, N. Chaoui, J. Photochem. Photobiol. A: Chem. 167 (2004) 49.
- [2] M. Karkmaz, E. Puzenat, C. Guillard, J.M. Herrmann, Appl. Catal. B: Environ. 51 (2004) 183.
- [3] P.V.A. Padmanabhan, K.P. Sreekumar, T.K. Thiyagarajan, R.U. Satpute, K. Bhanumurthy, P. Sengupta, G.K. Dey, K.G.K. Warriar, Vacuum 80 (2006) 1252.
- [4] K.T. Chung, C.E. Cerniglia, Mutat. Res. 277 (1992) 201.
- [5] S. Gomes de Moraes, R.S. Freire, N. Durán, Chemosphere 40 (2000) 369.
- [6] I.K. Konstantinou, T.A. Albanis, Appl. Catal. B: Environ. 49 (2004) 1, and references therein.
- [7] B. O'Regan, J. Moser, M. Anderson, M. Gratzel, J. Phys. Chem. 94 (1990) 8720.
- [8] S. Sodergren, A. Hagfeldt, J. Olsson, S.E. Lindquist, J. Phys. Chem. 98 (1994) 5552.
- [9] Y. Bessekhoud, D. Robert, J.V. Weber, J. Photochem. Photobiol. A: Chem. 163 (2004) 569.
- [10] Y. Bessekhoud, D. Robert, J.-V. Weber, Catal. Today 101 (2005) 315.
- [11] Y. Bessekhoud, N. Chaoui, M. Trzpit, N. Ghazzal, D. Robert, J.V. Weber, J. Photochem. Photobiol. A: Chem. 183 (2006) 218.
- [12] S.-M. Yang, Z.-S. Wang, C.-H. Huang, Synth. Met. 123 (2001) 267.
- [13] J.S. Hong, D.S. Choi, M.G. Kang, D. Kim, K.-J. Kim, J. Photochem. Photobiol. A: Chem. 143 (2001) 87.
- [14] S. Saadi, A. Bouguelia, M. Trari, Solar Energy 80 (2006) 272.
- [15] Y.J. Yang, L.Y. He, Electrochem. Acta 50 (2005) 3581.
- [16] S. Kumar, Z.H. Khan, M.A. Majeed Khan, M. Husain, Curr. Appl. Phys. 5 (2005) 561.
- [17] F. Zhang, J. Zhao, T. Shen, H. Hidaka, E. Pelizzetti, N. Serpone, Appl. Catal. B: Environ. 15 (1998) 147.
- [18] D. Fompeydie, F.O. Nur, P. Levillain, Bull. Soc. Chem. Fresen. (1979) 1–375.
- [19] J. Zhao, H. Hidaka, A. Takamura, E. Pelizzetti, N. Serpone, Langmuir 9 (1989) 1646.